

Library copy
RA A78 L127

UNCL

Copy 44
RM SL57D30

CONFIDENTIAL

C2

NACA

RESEARCH MEMORANDUM

for the

Bureau of Aeronautics, Department of the Navy

EFFECTS OF INLET MODIFICATION AND ROCKET-RACK EXTENSION ON
THE LONGITUDINAL TRIM AND LOW-LIFT DRAG OF THE DOUGLAS
F5D-1 AIRPLANE AS OBTAINED WITH A 0.125-SCALE
ROCKET-BOOSTED MODEL BETWEEN MACH
NUMBERS OF 0.81 AND 1.64

TEC NO. NACA AD 399

By Earl C. Hastings, Jr., and Waldo L. Dickens

Langley Aeronautical Laboratory
Langley Field, Va.

LIBRARY COPY

APR 30 1957

CLASSIFIED DOCUMENT

This material contains information affecting the National Defense of the United States within the meaning of the espionage laws, Title 18, U.S.C., Secs. 793 and 794, the transmission or revelation of which in any manner to an unauthorized person is prohibited by law.

LANGLEY AERONAUTICAL LABORATORY
LIBRARY, NACA
LANGLEY FIELD, VIRGINIA

NATIONAL ADVISORY COMMITTEE FOR AERONAUTICS

WASHINGTON
APR 29 1957

CONFIDENTIAL

UNCL
UNAVAILABLE

Library copy
NA. A73 L127

UNC

Copy 46
RM ST 57D30

CONFIDENTIAL



RESEARCH MEMORANDUM

for the

Bureau of Aeronautics, Department of the Navy

EFFECTS OF INLET MODIFICATION AND ROCKET-RACK EXTENSION ON
THE LONGITUDINAL TRIM AND LOW-LIFT DRAG OF THE DOUGLAS
F5D-1 AIRPLANE AS OBTAINED WITH A 0.125-SCALE
ROCKET-BOOSTED MODEL BETWEEN MACH
NUMBERS OF 0.81 AND 1.64

TED NO. NACA AD 399

By Earl C. Hastings, Jr., and Waldo L. Dickens

Langley Aeroneautical Laboratory
Langley Field, Va.

LIBRARY COPY

APR 30 1957

CLASSIFIED DOCUMENT

This material contains information affecting the National Defense of the United States within the meaning of the espionage laws, Title 18, U.S.C., Secs. 793 and 794, the transmission or revelation of which in any manner to an unauthorized person is prohibited by law.

LANGLEY AERONAUTICAL LABORATORY
LIBRARY, NACA
LANGLEY FIELD, VIRGINIA

NATIONAL ADVISORY COMMITTEE FOR AERONAUTICS

WASHINGTON

APR 29 1957

CONFIDENTIAL

NATIONAL ADVISORY COMMITTEE FOR AERONAUTICS

RESEARCH MEMORANDUM

for the

Bureau of Aeronautics, Department of the Navy

EFFECTS OF INLET MODIFICATION AND ROCKET-RACK EXTENSION ON
THE LONGITUDINAL TRIM AND LOW-LIFT DRAG OF THE DOUGLAS
F5D-1 AIRPLANE AS OBTAINED WITH A 0.125-SCALE
ROCKET-BOOSTED MODEL BETWEEN MACH

NUMBERS OF 0.81 AND 1.64

TED NO. NACA AD 399

By Earl C. Hastings, Jr., and Waldo L. Dickens

SUMMARY

A flight investigation was conducted to determine the effects of an inlet modification and rocket-rack extension on the longitudinal trim and low-lift drag of the Douglas F5D-1 airplane. The investigation was conducted with a 0.125-scale rocket-boosted model which was flight tested at the Langley Pilotless Aircraft Research Station at Wallops Island, Va.

Results indicate that the combined effects of the modified inlet and fully extended rocket racks on the trim lift coefficient and trim angle of attack were small between Mach numbers of 0.94 and 1.57. Between Mach numbers of 1.10 and 1.57 there was an average increase in drag coefficient of about 0.005 for the model with modified inlet and extended rocket racks. The change in drag coefficient due to the inlet modification alone is small between Mach numbers of 1.59 and 1.64.

INTRODUCTION

This paper presents the results of the last phase of a program which has been conducted by the National Advisory Committee for Aeronautics with rocket-boosted models of the Douglas F4D-1 and Douglas F5D-1 airplanes.

[Redacted]

Reference 1 is a summary of the results of the F4D-1 investigation and reference 2 presents the development and test results for one version of the F5D-1.

The purpose of the investigation reported herein was twofold: First, to determine the drag increment and longitudinal-trim change associated with the extension of the airplane rocket racks at supersonic speeds, and second, to determine the effects on low-lift drag resulting from a modified inlet and inlet lip by comparison with the data of reference 2 where the rocket racks were closed.

SYMBOLS

A	cross-sectional area, sq ft
a_l/g	longitudinal-accelerometer reading
a_n/g	normal-accelerometer reading
\bar{c}	mean aerodynamic chord, ft
C_c	chord-force coefficient, positive in rearward direction, $-\frac{a_l}{g} \frac{W}{qS}$
C_D	drag coefficient
$C_{D,tot}$	total drag coefficient, $C_c \cos \alpha + C_N \sin \alpha$
C_L	lift coefficient, $C_N \cos \alpha - C_c \sin \alpha$
C_N	normal-force coefficient, positive toward top of model, $\frac{a_n}{g} \frac{W}{qS}$
g	acceleration due to gravity, 32.2 ft/sec ²
l	length, ft
M	Mach number
w/w_∞	ratio of total mass flow through ducts to mass flow at free-stream conditions passing through an area equal to total inlet-capture area
p_t	total pressure, lb/sq ft

p	static pressure, lb/sq ft
q	dynamic pressure, lb/sq ft
R	Reynolds number
r	radius, ft
S	total wing area, sq ft
t	time, sec
V	velocity, ft/sec
W	weight, lb
x	station measured from nose, ft
α	angle of attack, deg
γ	flight-path angle, deg, or ratio of specific heats

Subscripts:

b	base
e	duct exit
i	duct inlet (capture)
∞	free stream
ext	external
int	internal
tot	total

MODEL AND APPARATUS

Model

A three-view drawing of the 0.125-scale model tested is presented as figure 1 and a photograph of the model is shown as figure 2. Table I presents the physical characteristics of the model and figure 3 shows

the normal cross-sectional-area distribution and equivalent body-of-revolution of the model. In order to show the inlet and inlet-lip modifications incorporated in this version of the Douglas F5D-1 airplane, figure 1 shows the inlet configuration of the previous version (configuration 2 of ref. 2) for comparison. There were no changes made in any of the internal duct lines or in the longitudinal location of the inlets on the body. Figure 1 does show, however, that the original inlet was thinned down by reducing the thickness of the area around the duct. As a result, the modified inlets were externally smaller and less sharply diverging than the original inlets and had lips that were less blunt. In both cases, however, the inlet lips themselves were of a rounded, subsonic design. The change in normal cross-sectional-area distribution due to the inlet modification can also be seen in figure 3(b) but this increment is too small to be seen in the equivalent-body-of-revolution plot of figure 3(a).

Fuselage construction consisted of an internal steel thrust tube with mahogany and fiber-glass fairings making up the external contours. The nose hatch was a removable fiber-glass casting that housed the telemeter equipment. Access to other instrumentation was provided by removable fiber-glass hatches on the top and bottom of the model. Space was provided also in the fuselage for a smoke tank to aid radar tracking.

The construction of the modified delta wing was a box beam made of spanwise steel spars with aluminum-alloy cover plates. The exterior surfaces of the wings and fillets were molded plastic and the vertical tail was made of machined aluminum alloy.

The model rocket racks were scaled to duplicate the full-scale airplane in their location, size, and movement. (See figs. 1, 4, and 5.) The racks were designed to operate in a square-wave motion between the fully closed and fully extended position by using an electric motor to supply the torque and a programmed cam for the desired timing sequence. Because of the high longitudinal loads involved during the boosted phase of the flight, the system was designed to operate only after model-booster separation. This was accomplished by installing a switch in the base of the model to keep the rocket-rack circuit open during boost.

In order to present external drag it was necessary to instrument the model for internal and base drag. The rear of the duct was choked with a minimum section, and a total-pressure rake consisting of six probes was installed near this section so that internal drag could be determined at Mach numbers greater than 1.00. Base static-pressure measurements were made by using four static-pressure orifices spaced 90° apart around the base annulus and manifolded together inside the model.

The model was boosted to a Mach number of about 1.64 by two 6.25-inch-diameter ABL Deacon rocket motors which were timed to fire simultaneously.

Figure 6 is a photograph of the model-booster combination. After the rocket motors had stopped thrusting, the model separated from the booster and the data presented herein were obtained during the coasting phase of the flight.

Apparatus

The quantities necessary to determine the drag at low lift and the longitudinal trim characteristics were transmitted to a ground receiving station by an internal telemeter system. The telemetered channels of information recorded were free-stream and duct total pressure, angle of attack, longitudinal and normal accelerations, base static pressure, and rocket-rack position.

Free-stream static pressure and temperature were obtained from a rawinsonde released at time of firing. Ground equipment consisting of a CW Doppler radar unit and an NACA modified SCR-584 tracking-radar unit were used to determine model velocity and position in space, respectively.

ANALYSIS OF DATA

In addition to values of total drag coefficient obtained from the measured telemeter data the CW Doppler radar values of velocity obtained during this test can be used to give an additional set of total-drag values. By differentiating this velocity with respect to time and adding the flight-path component of weight to obtain the drag deceleration, the total drag coefficient can be found by the following relationship:

$$C_{D,tot} = - \left(\frac{dV}{dt} + g \sin \gamma \right) \frac{W}{qSg}$$

A more complete discussion of this method of analysis and the equipment involved can be found in reference 3.

Base and internal drag coefficients were determined from telemeter quantities measured during the flight. Static-pressure measurements made on the model base annulus were used to calculate base drag coefficient from the equation

$$C_{D,b} = \frac{-(p_b - p_o)(\text{Base area})}{qS}$$

Internal drag coefficient was computed by the method of reference⁴ expressed in terms of the equation

$$C_{D,int} = \frac{2A_e}{S} \left[\frac{w}{w_\infty} \left(\frac{A_i}{A_e} \right) - \frac{p_e (M_e)}{p_\infty (M_\infty)}^2 - \left(\frac{p_e - p_\infty}{\gamma p_\infty M_\infty^2} \right) \right]$$

where γ is the ratio of specific heats. With the instrumentation used in this investigation all of the quantities necessary to determine internal drag coefficient at Mach numbers less than 1.00 were not measured. Estimates were made at subsonic speeds, however, by assuming that the values of duct-exit static pressure were the same as the measured values of base static pressure. Experience with models having similar duct-exit and base configurations has shown that this assumption is valid and reasonable estimates usually result.

External drag coefficients were determined by subtracting $C_{P,int}$ and $C_{D,b}$ from the faired values of $C_{D,tot}$. Inasmuch as these values of $C_{D,ext}$ were obtained at low trim lift coefficients and trim angles of attack they represent essentially the minimum drag of the model for the test conditions discussed herein.

ACCURACY

The following table presents what is felt to be reasonable values of the accuracy of the various quantities and coefficients presented in this paper. Where possible, these values have been obtained from agreement between comparative data in this or in similar tests. Where the accuracy could not be obtained from a comparison of data the values have been estimated on the basis of instrument error.

Quantity	Accuracy at -	
	M = 0.80	M = 1.64
ΔM	0.020	0.010
$\Delta C_{D,tot}$	0.0020	0.0015
$\Delta C_{D,b}$	0.0003	0.0003
$\Delta C_{D,int}$	-----	0.0003
$\Delta C_{L,trim}$	0.030	0.010
$\Delta \alpha_{trim}$, deg	0.30	0.30

As mentioned in the section entitled "Analysis of Data" the internal drag coefficient could not be measured at subsonic speeds; therefore, no value of accuracy of $\Delta C_{D,int}$ is presented at $M = 0.80$. In order to increase the accuracy of this coefficient at low supersonic Mach numbers, however, dual-range total-pressure cells were used to measure the duct-exit total pressure so that at $M = 1.00$ the accuracy of $\Delta C_{D,int}$ is about 0.0004.

RESULTS AND DISCUSSION

Test Conditions

The variation of test Reynolds number (based on the wing mean aerodynamic chord) with Mach number is shown in figure 7, and the mass-flow ratio during the test is shown in figure 8. By operating in the range of mass-flow ratio shown in figure 8 the model closely duplicated the mass-flow requirements of the full-scale airplane at probable operational Mach numbers and altitudes.

Figure 9 presents the total-pressure recovery of the duct. These values should be considered qualitative because they were measured near the duct exit and therefore represent the loss in total pressure relative to the duct exit rather than the engine face.

The position of the rocket racks during the test is shown in figure 10. This figure shows that the racks did not function properly and as a result the incremental drag difference due to the effect of the inlet modification alone can be determined only for Mach numbers between $M = 1.59$ and 1.64 where the racks are fully closed. Between $M = 0.94$ and $M = 1.57$, however, the racks are essentially fully extended and the effects of the rack extension on the longitudinal trim of the model can be determined.

Longitudinal Trim

Figures 11 and 12 present the variations with Mach number of $C_{L,trim}$ and α_{trim} , respectively, for the model of the present test and the model from the test of reference 2. The model of reference 2 had the original inlets, a center-of-gravity location at 0.181C, and the rocket racks fully closed. A comparison of the data presented in figure 11 shows that between $M = 0.81$ and $M = 0.92$ when the racks are only about 44 percent extended there is a negative shift of 0.042 in $C_{L,trim}$. For the supersonic Mach numbers of the test when the racks are essentially fully extended, the

increment in $C_{L,trim}$ is a small negative shift which decreases with increasing Mach number until, between $M = 1.40$ and 1.57 , the fully extended rocket racks have no effect upon $C_{L,trim}$. By comparing the data of figure 11 in the Mach number range where the rockets racks of the present test were closed ($M = 1.59$ to 1.64) it can be seen that the inlet modifications alone have no effect on the value of $C_{L,trim}$ between these Mach numbers.

A comparison of the values of α_{trim} in figure 12 shows that there is a small negative shift of 0.37° due to the rocket racks being extended at about the 44-percent location between $M = 0.81$ and $M = 0.92$. At Mach numbers greater than 1.00 , however, the change in α_{trim} due to fully extended racks is a positive shift having its greatest influence at about $M = 1.37$ where the shift in α_{trim} due to extended racks is about 0.55° . Between $M = 1.59$ and $M = 1.64$ the racks are closed and the effects of the inlet redesign alone on α_{trim} in this Mach number range is seen to be negligible.

Figures 11 and 12 indicate that, between $M = 0.97$ and $M = 1.54$ when rocket racks are fully extended, the values of $C_{L,trim}$ are slightly negative while α_{trim} is positive. This condition does not exist for the test of reference 2 in which the racks were closed. Apparently the pressure field created by the extended racks counteracts the positive lift increment associated with positive values of α_{trim} so that the resultant $C_{L,trim}$ is negative. The abrupt changes in $C_{L,trim}$ and α_{trim} which occur between about $M = 0.94$ and $M = 0.97$ are transonic effects rather than effects caused by rack movement inasmuch as the rack position is constant from $M = 0.94$ to $M = 1.57$. An examination of the telemeter record shows that these changes take place while the racks are stationary. In general, the changes in the longitudinal-trim data in figures 11 and 12 caused by the full rocket-rack extension and inlet modification between $M = 0.94$ and $M = 1.57$ are shown to be small.

Drag

Figure 13 presents $C_{D,tot}$ from the telemeter and the CW Doppler tracking-radar data. Agreement between the two sources of data is very good at the higher Mach numbers of the test. Inasmuch as drag obtained from tracking-radar data has usually proved to be more unreliable than telemeter data at the lower Mach numbers for this type of test, the faired values of $C_{D,tot}$ in figure 13 are based upon telemeter data alone below $M = 1.28$.

Measured values of $C_{D,b}$ and $C_{D,int}$ and estimated subsonic values of $C_{D,int}$ are shown as functions of Mach number in figure 14. These measured data were in excellent agreement with those of reference 2 although this comparison is not made in figure 14 for the sake of figure clarity. Throughout the Mach number range of the test, $C_{D,int}$ is nearly constant at 0.0007 and $C_{D,b}$ increases from about 0 at subsonic speeds to about 0.0015 at Mach numbers above 1.20.

The external drag coefficient of the present test is compared with that of reference 2 in figure 15 to show the effects of rocket-rack extension and inlet modification. Because of the wide-range instrument used in the measurements of duct total pressure in reference 2, the subsonic estimates of $C_{D,int}$ from reference 2 were believed to be unreliable. As a result, values of $C_{D,ext}$ from reference 2 were not corrected for $C_{D,int}$ below $M = 1.00$, whereas the data of the present test is corrected for the estimated values of $C_{D,int}$ between $M = 0.81$ and 1.00. This should be kept in mind when comparing values of $C_{D,ext}$ from figure 15 at Mach numbers below $M = 1.00$.

When the rocket racks move from 47 percent extended to 94 percent extended between $M = 0.93$ and $M = 0.94$ there is an increase of 0.0010 in $C_{D,ext}$. The drag-rise Mach number (the Mach number at which $dC_D/dM = 0.10$) with the rocket racks 94 percent extended occurs at $M = 0.96$. Between $M = 1.10$ and $M = 1.57$, $C_{D,ext}$ is constant at 0.028 with the racks essentially fully extended. This represents an increase in $C_{D,ext}$ due to inlet modification and rocket-rack extension of 0.003 at $M = 1.10$ and 0.005 at $M = 1.25$. From $M = 1.25$ to $M = 1.57$ the increase in $C_{D,ext}$ due to inlet modification and rocket-rack extension remains a constant value of 0.005. When the rocket racks are fully closed between $M = 1.59$ and $M = 1.64$ the effects of the inlet modification alone on the drag of the configuration can be determined. Figure 15 shows that the change in $C_{D,ext}$ due to the inlet modification is so small that it is within the accuracy of the data between $M = 1.59$ and $M = 1.64$.

CONCLUSIONS

A flight investigation was conducted with a 0.125-scale rocket-boosted model of the Douglas F5D-1 airplane to determine the effects produced by rocket-rack extension and an inlet modification on longitudinal trim and external drag. The following conclusions are indicated:

1. The changes produced in trim lift coefficient and trim angle of attack due to inlet modifications and full rocket-rack extensions were small between Mach numbers of 0.94 and 1.57.
2. With the rocket racks fully extended and the revised inlet incorporated the drag-rise Mach number was 0.96. Between Mach numbers of 1.10 and 1.57 the external drag coefficient was constant at 0.028 (an average increase of about 0.005 over that of the model with the original inlets and closed rocket racks).
3. Between Mach numbers of 1.59 and 1.64 the change in external drag coefficient due to inlet modification alone was small.

Langley Aeronautical Laboratory,
National Advisory Committee for Aeronautics,
Langley Field, Va., April 11, 1957.

Earl C. Hastings Jr.
Earl C. Hastings, Jr.
Aeronautical Research Engineer

Waldo L. Dickens
Waldo L. Dickens
Engineering Aid

Approved:

Joseph A. Shortal
Joseph A. Shortal
Chief of Pilotless Aircraft Research Division

sam

REFERENCES

1. Mitcham, Grady L., Blanchard, Willard S., Jr., and Hastings, Earl C., Jr.: Summary of Low-Lift Drag and Directional Stability Data From Rocket Models of the Douglas XF4D-1 Airplane With and Without External Stores and Rocket Packets at Mach Numbers From 0.8 to 1.38 - TED NO. NACA DE 349. NACA RM SL52G11, Bur. Aero., 1952.
2. Hastings, Earl C., Jr., and Mitcham, Grady L.: Comparison of the Minimum Drag of Two Versions of a Modified Delta-Wing Fighter As Obtained From Flight Tests of Rocket-Boosted Models and Equivalent Bodies Between Mach Numbers of 0.80 and 1.64. NACA RM L56E04, 1956.
3. Wallskog, Harvey A., and Hart, Roger G.: Investigation of the Drag of Blunt-Nosed Bodies of Revolution in Free Flight at Mach Numbers from 0.6 to 2.3. NACA RM L53D14a, 1953.
4. Faget, Maxime A., Watson, Raymond S., and Bartlett, Walter A., Jr.: Free-Jet Tests of a 6.5-Inch Diameter Ram-Jet Engine at Mach Numbers of 1.81 and 2.00. NACA RM L50L06, 1951.

TABLE I.- PHYSICAL CHARACTERISTICS OF A 0.125-SCALE MODEL
OF THE DOUGLAS F5D-1 AIRPLANE

Wing:

Area (total), sq ft	8.71
Span, ft	4.19
Aspect ratio	2.01
Mean aerodynamic chord, ft	2.28
Sweepback of leading edge, deg	52.5
Dihedral (relative to mean thickness line), deg	0.0
Taper ratio, (Tip chord)/(Root chord)	0.33
Airfoil section at root	NACA 0005 (modified)
Airfoil section at tip	NACA 0003.2 (modified)

Vertical tail:

Area (leading and trailing edges extended to center line) sq ft	1.49
Aspect ratio	2.89
Height (above fuselage center line), ft	1.47
Sweepback of leading edge, deg	51.7
Taper ratio, (Tip chord)/(Root chord)	0.40
Airfoil section at root	NACA 0005 (modified)
Airfoil section at tip	NACA 0003.2 (modified)

Ducts:

Total inlet-capture area, sq in.	9.45
Exit area, sq in.	8.60

Weight and balance:

Weight, lb	171.6
Wing loading, lb/sq ft	19.72
Center-of-gravity location, percent c	19.01
Moment of inertia in pitch, slug-ft ²	13.99

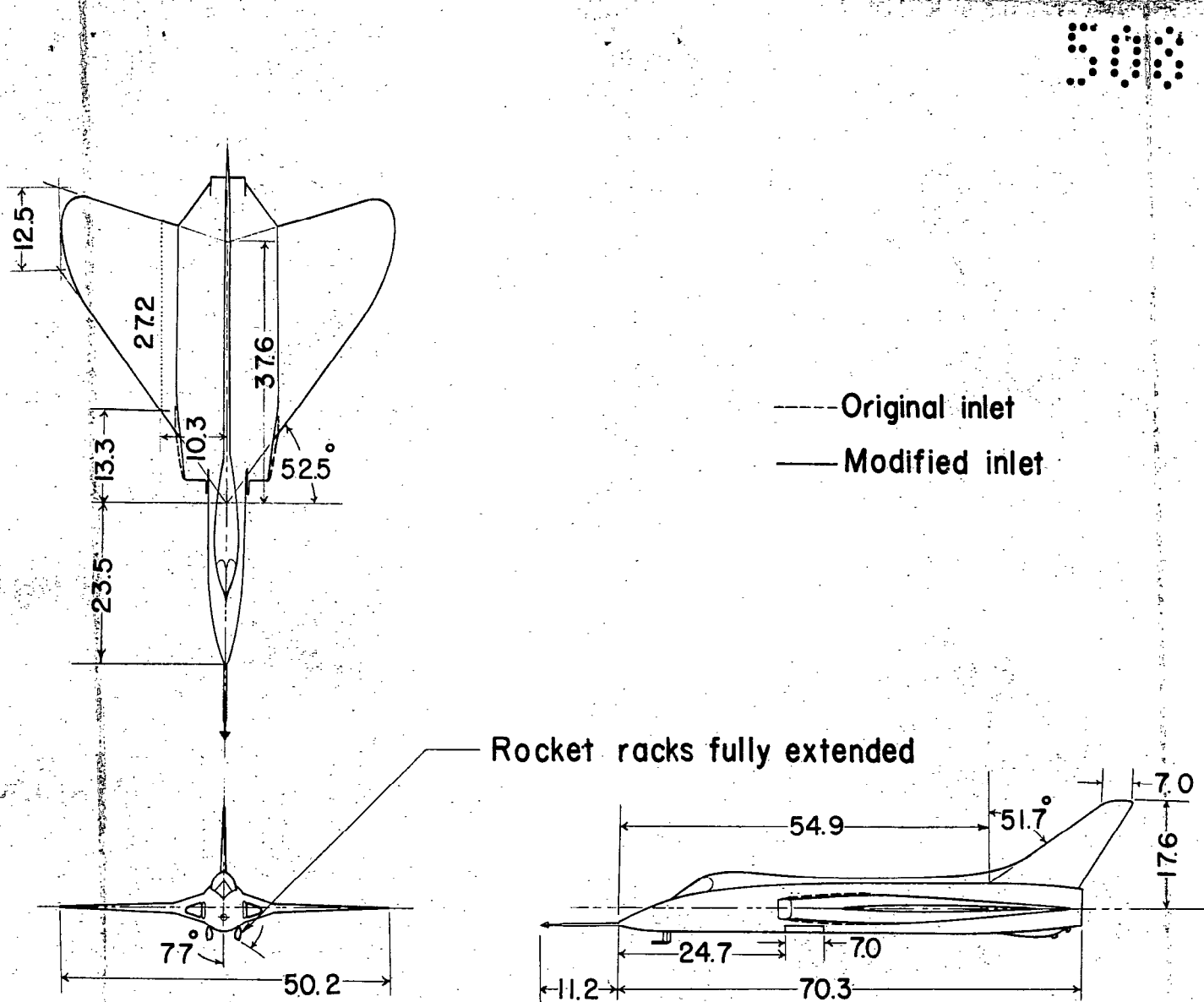


Figure 1.- Three-view drawing of the model. (All linear dimensions are in inches.)

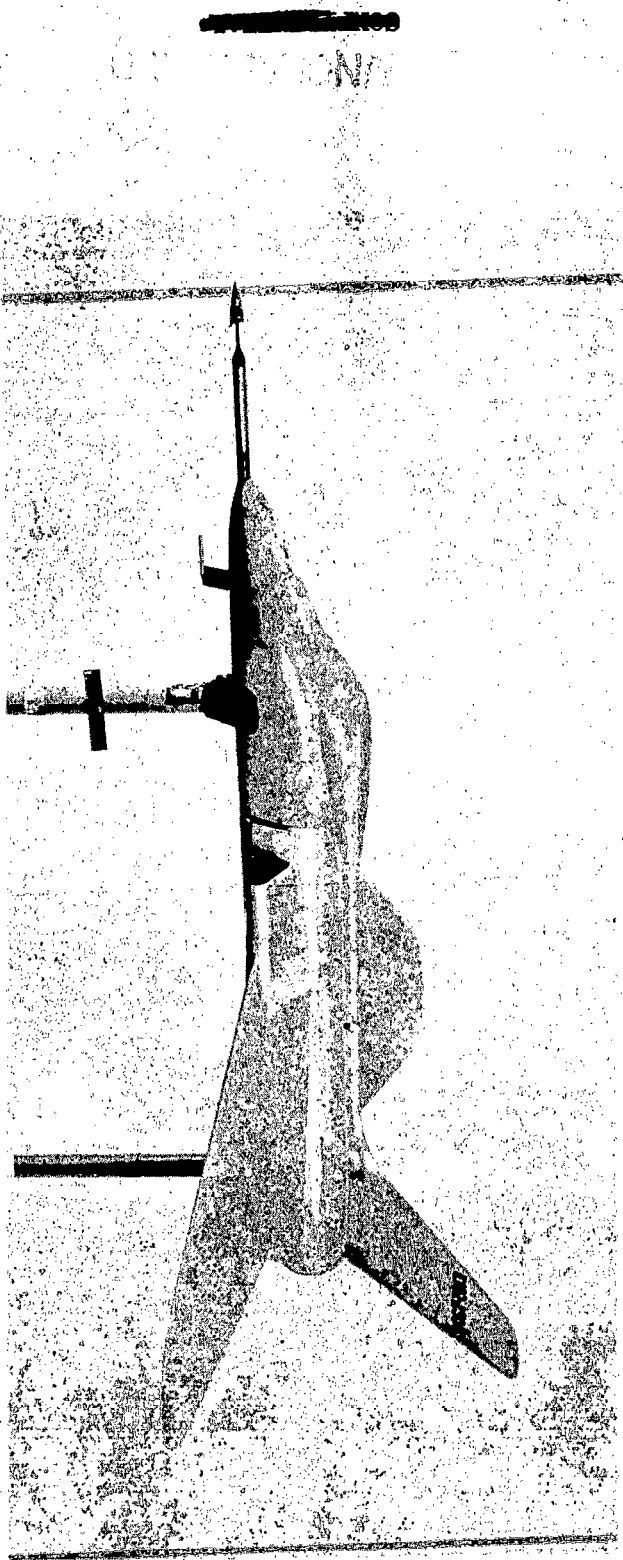
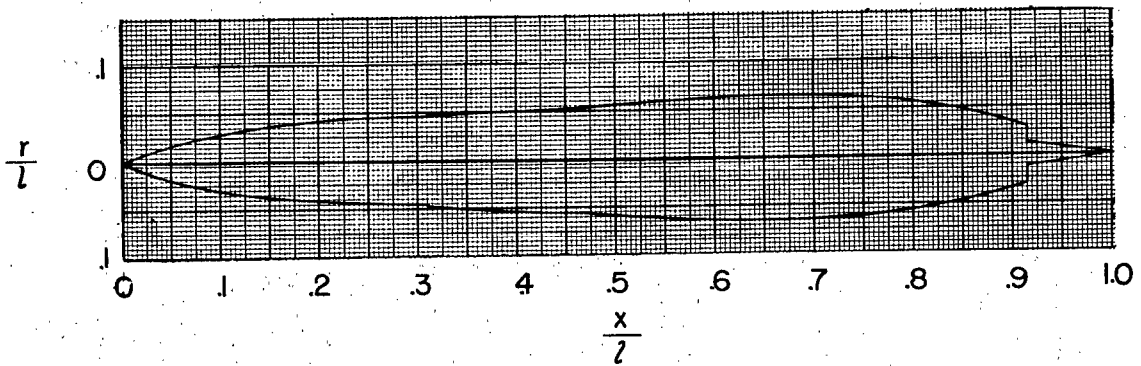


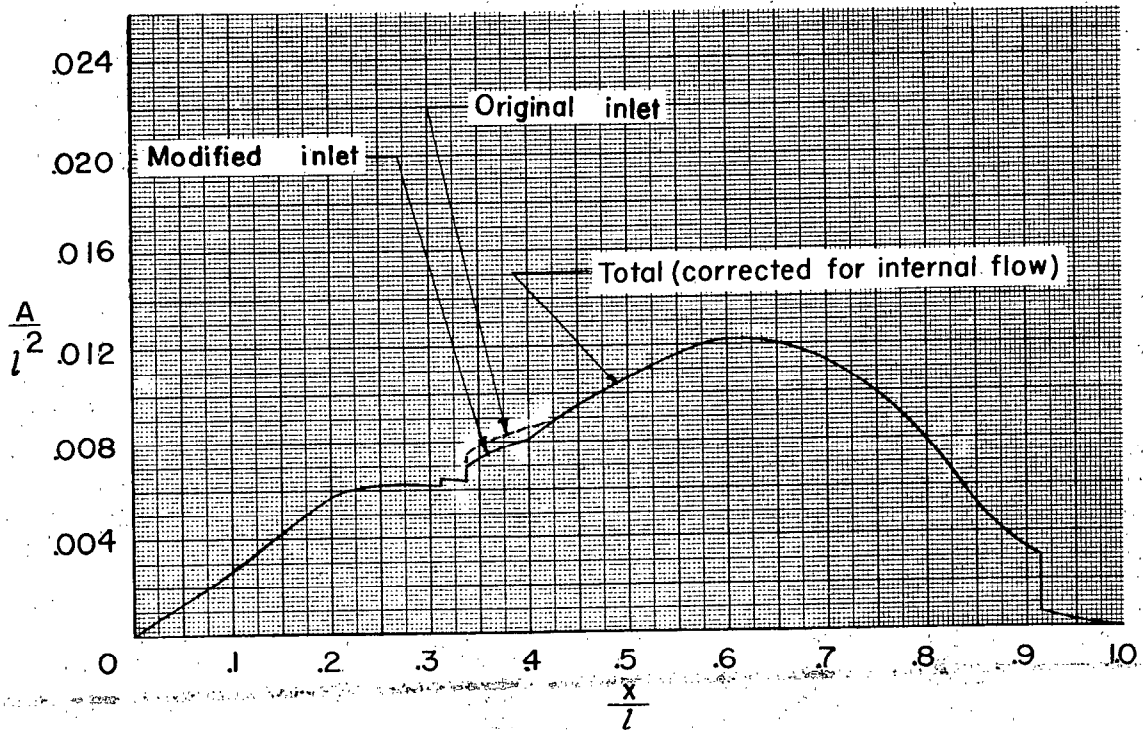
Figure 2.- Photograph of the model. I-96374

14

NACA RM SL57D30



(a) Equivalent body of revolution.



(b) Area distribution.

Figure 3.- Equivalent body of revolution and normal cross-sectional-area distribution of the model.

NACA RM SL57D30

16

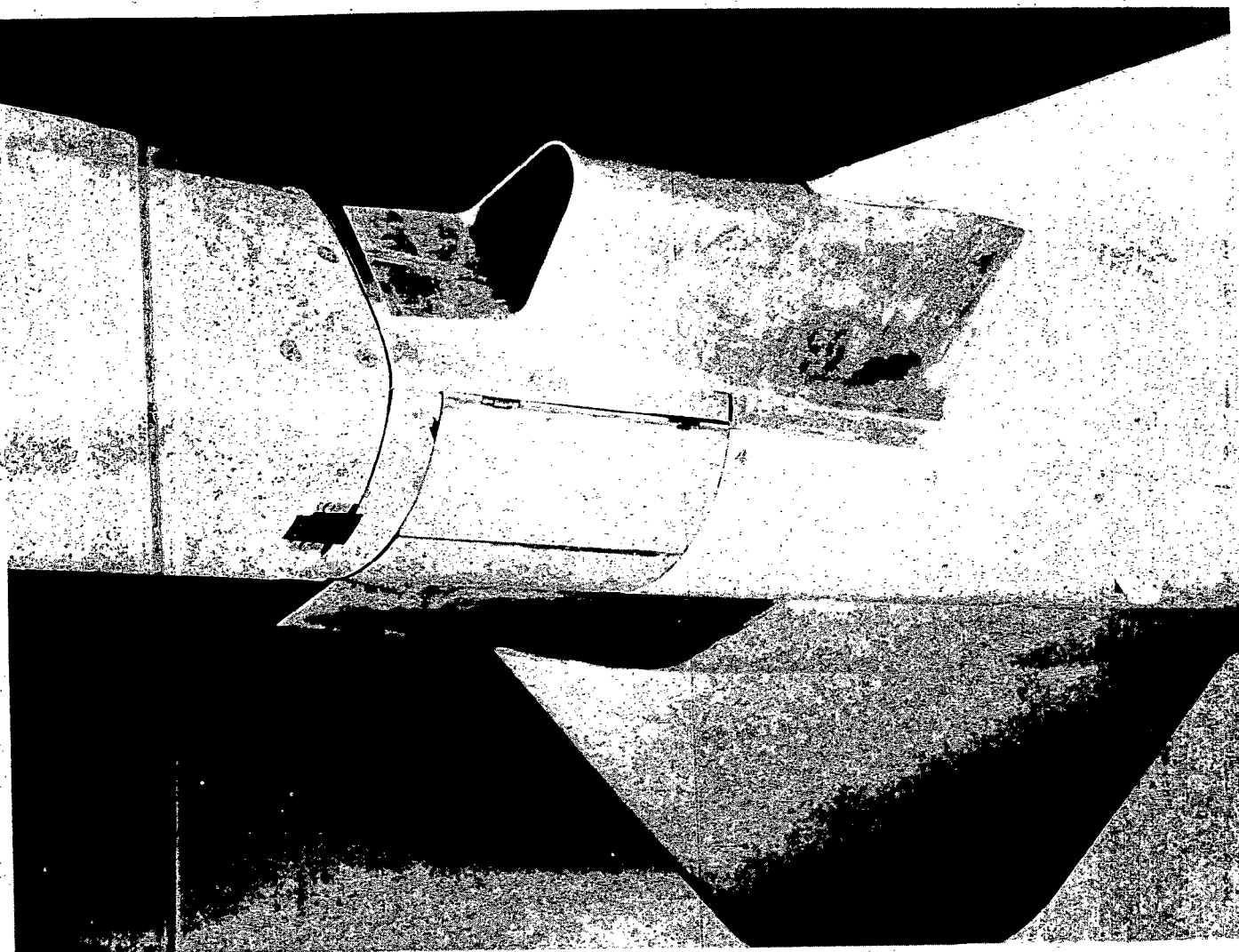
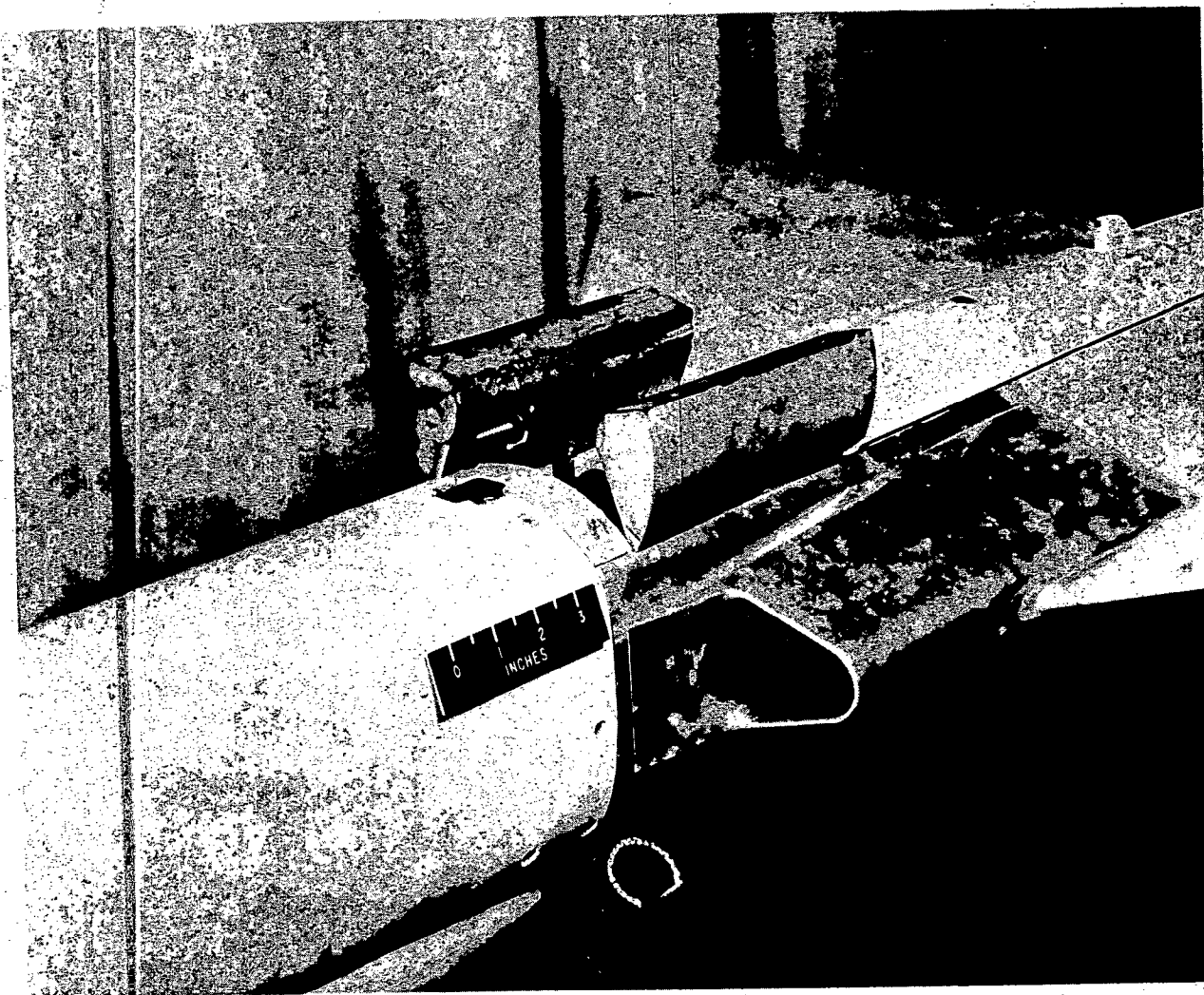


Figure 4.- Photograph of rocket racks in closed position. L-96376

50816

NACA RM SL57D30



L-96549

Figure 5.- Photograph of rocket racks in extended position.

NACA RM SL57D30

18

500

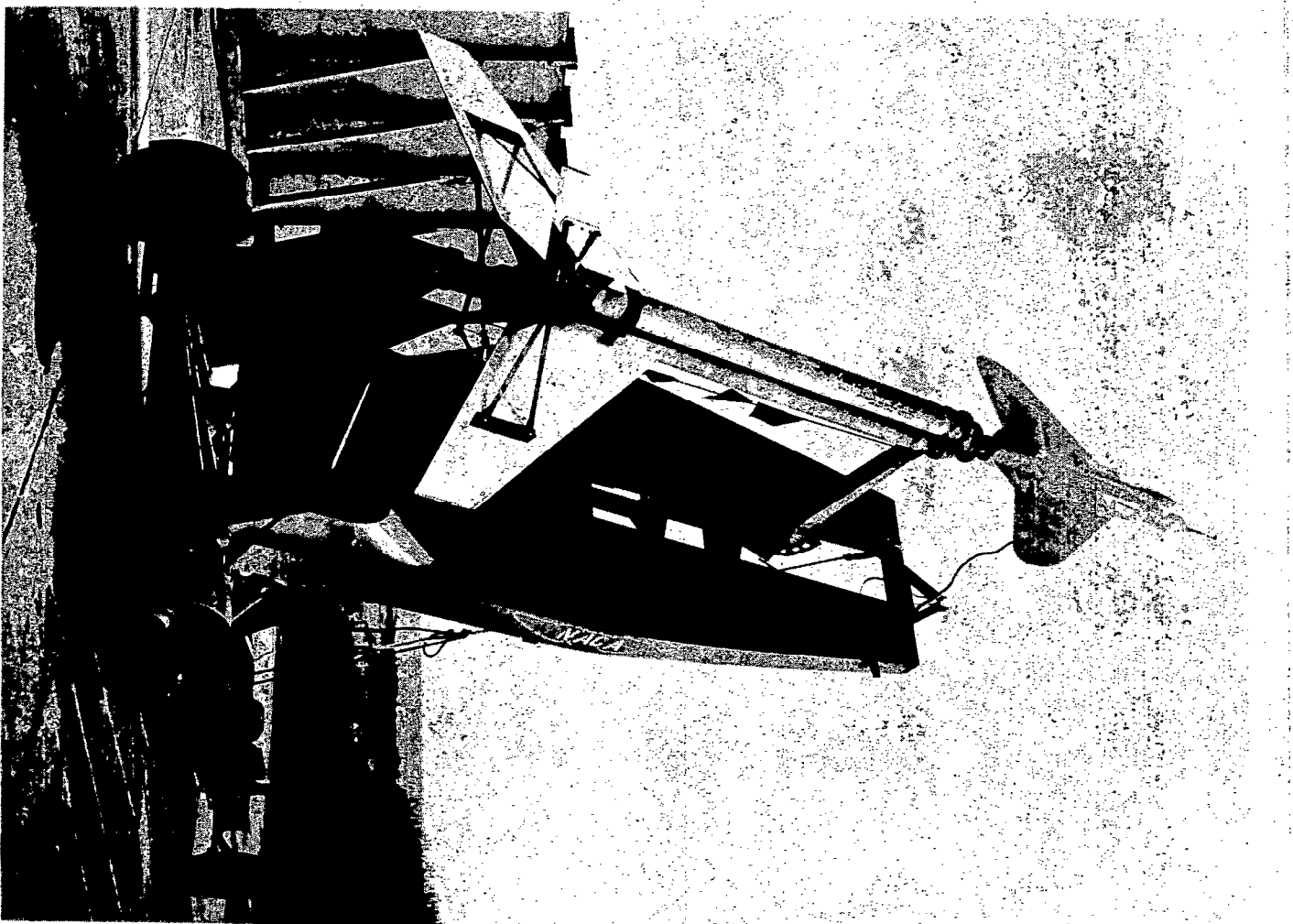


Figure 6.- Photograph of model-booster combination. L-96552

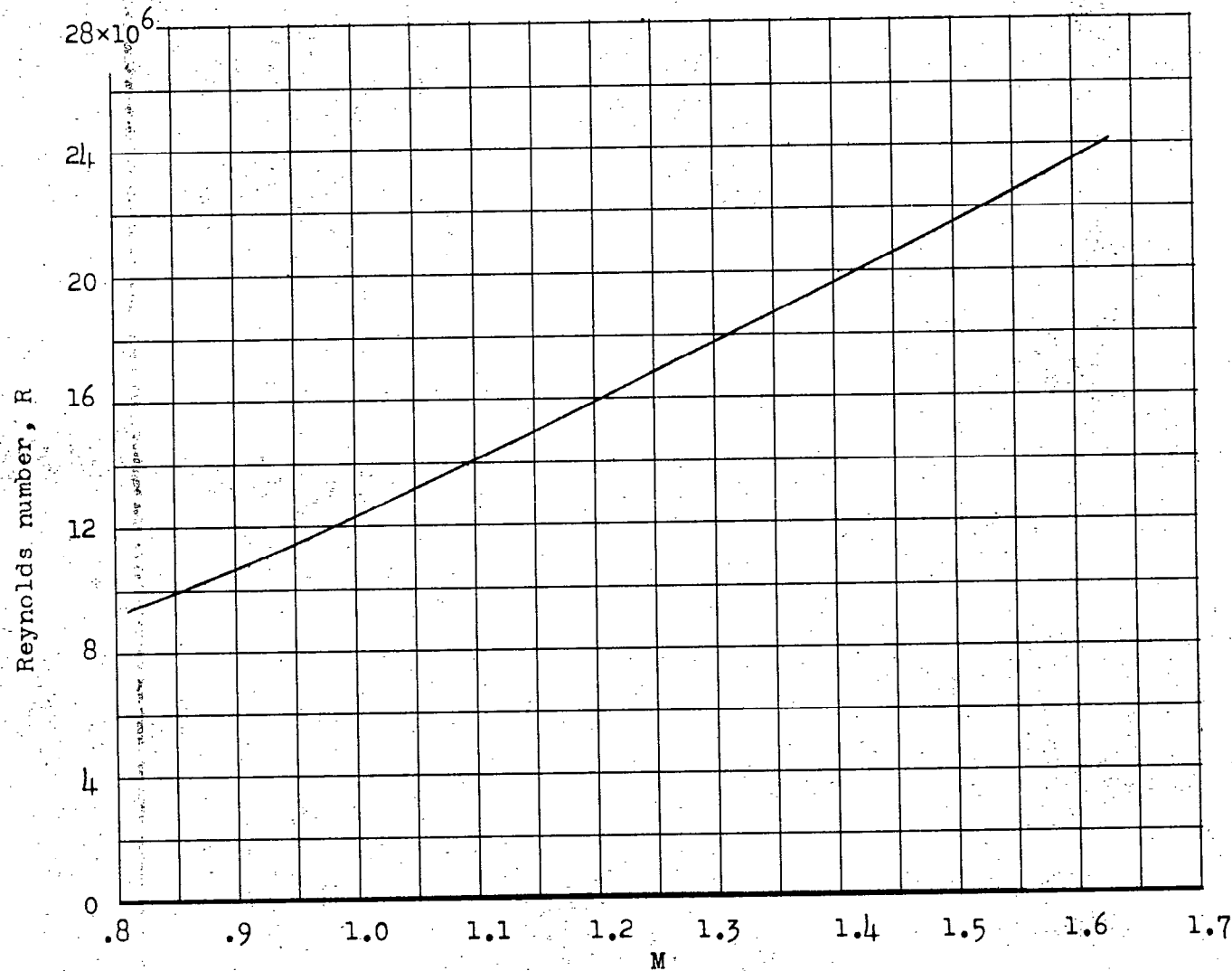


Figure 7.- Reynolds number based on a mean aerodynamic chord of 2.28 feet.

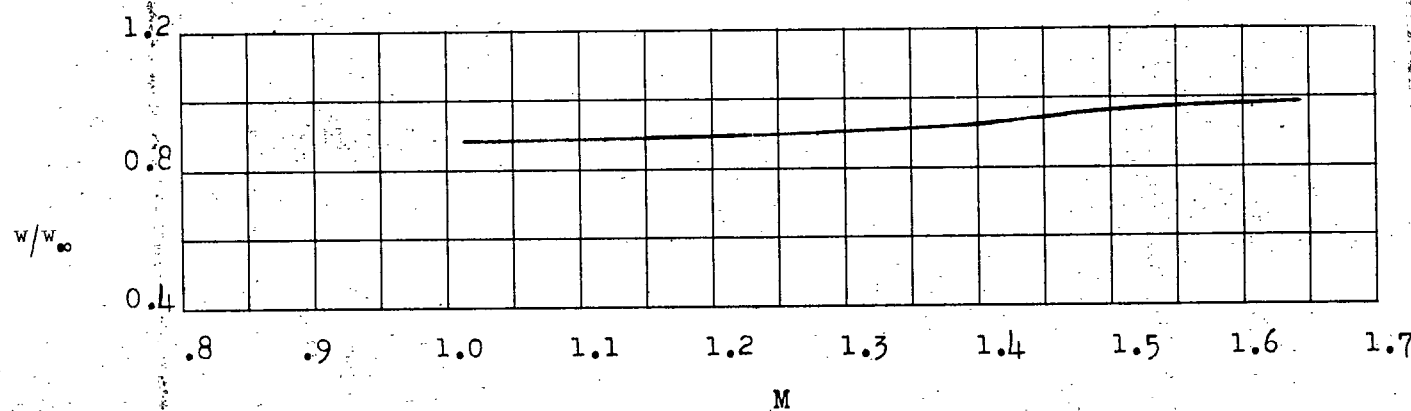


Figure 8.- Mass-flow ratio.

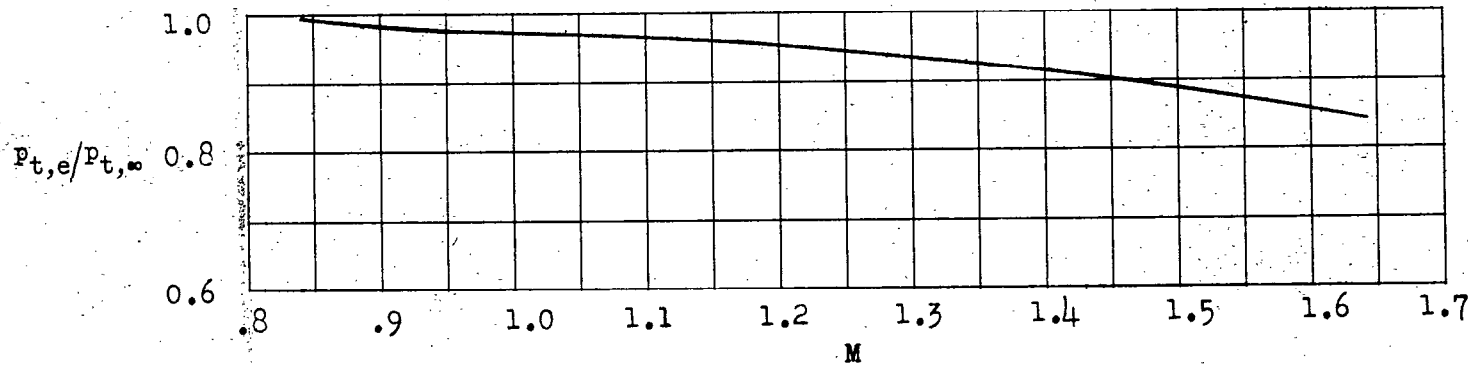


Figure 9.- Total-pressure recovery.

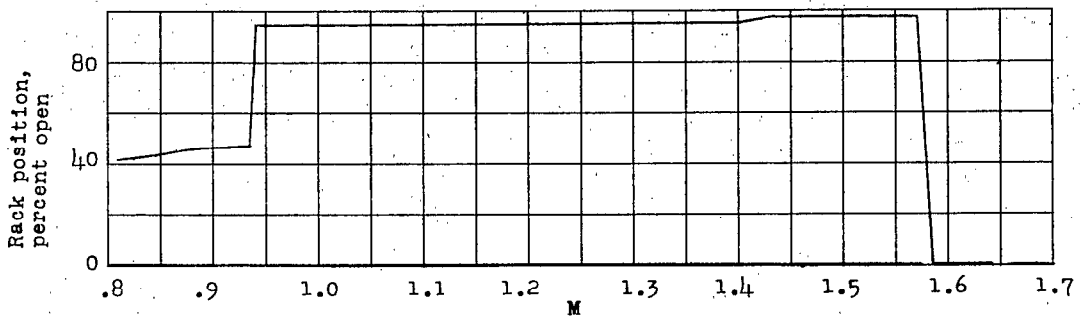


Figure 10.- Rocket-rack position.

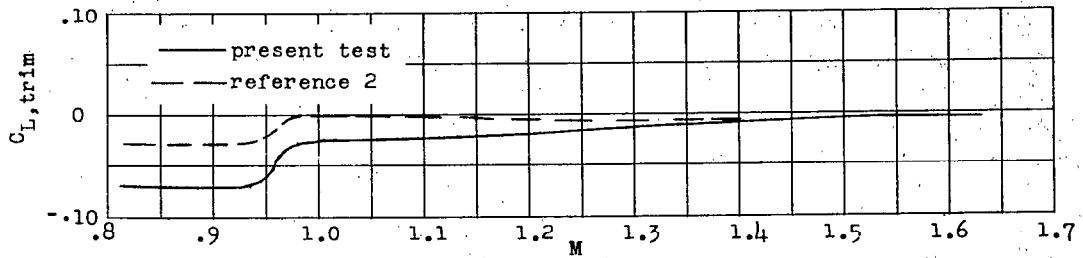
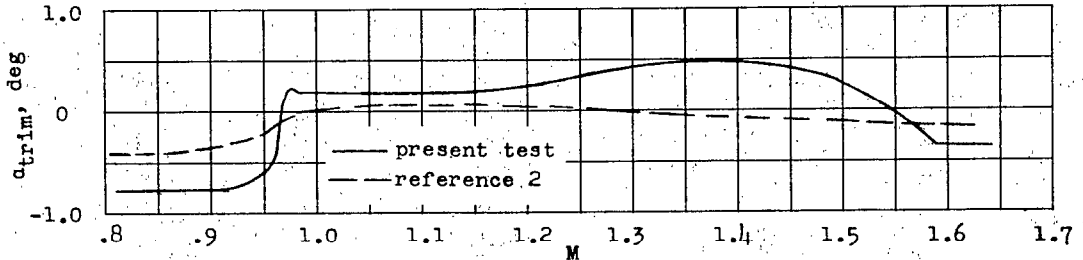


Figure 11.- Trim lift coefficient.



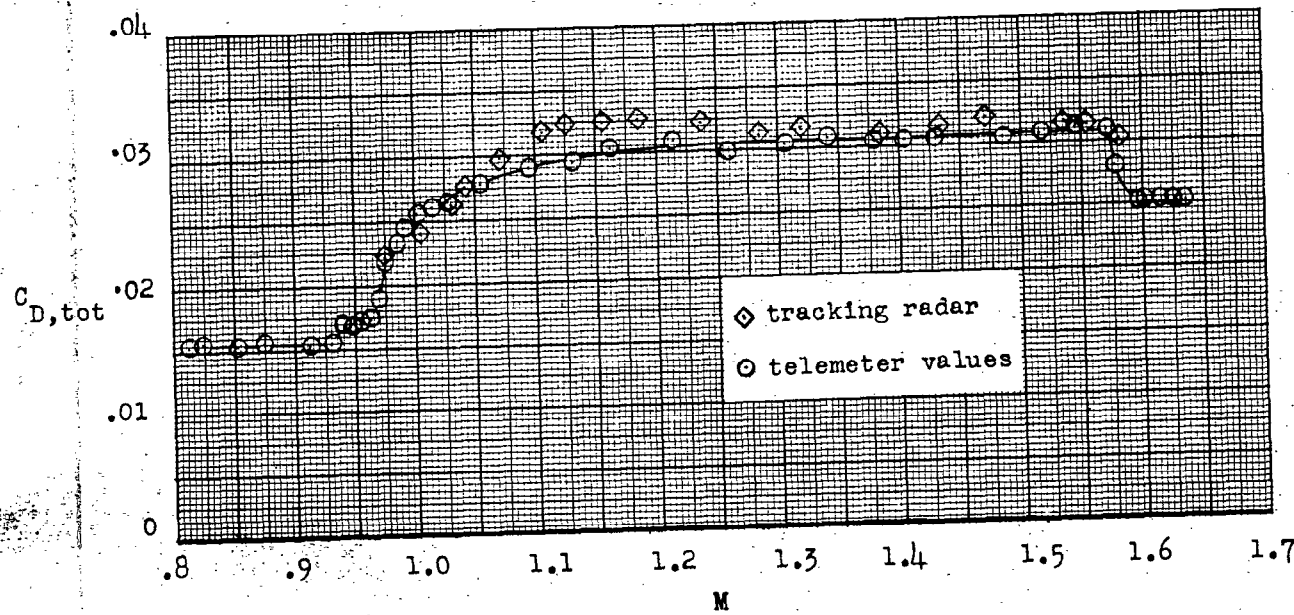


Figure 13.- Total drag coefficient.

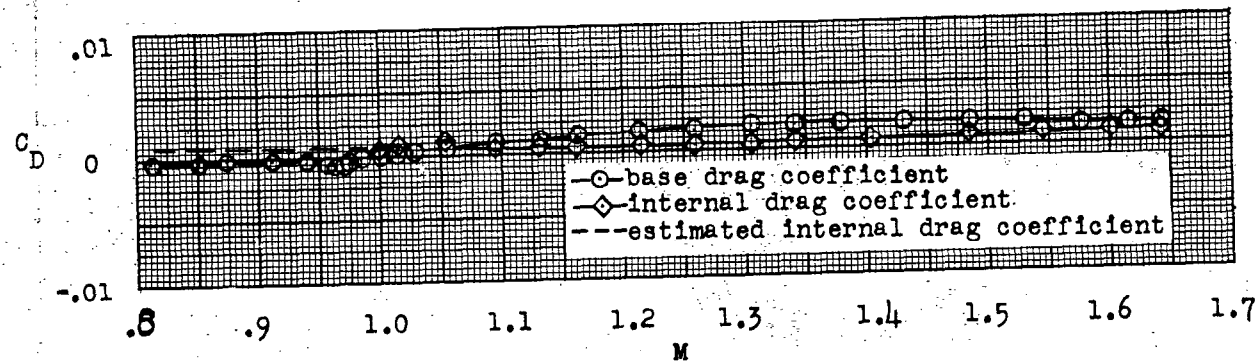


Figure 14.- Internal and base drag coefficients.

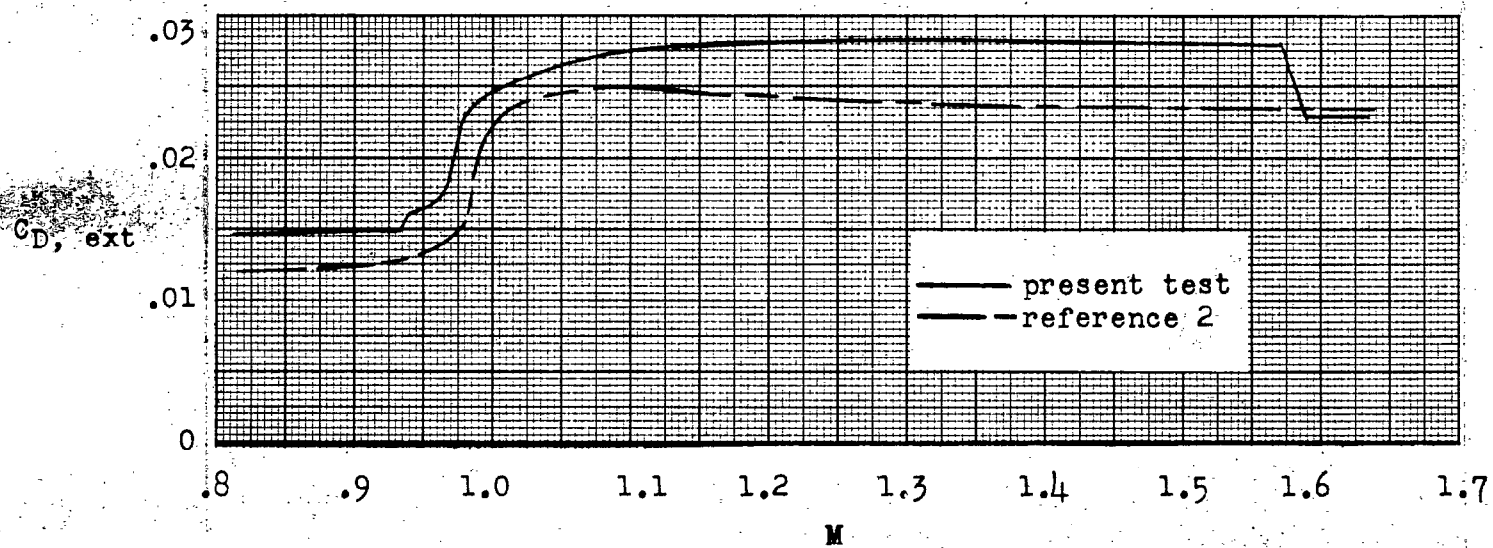


Figure 15.- External drag coefficient.

EFFECTS OF INLET MODIFICATION AND ROCKET-RACK EXTENSION ON
THE LONGITUDINAL TRIM AND LOW-LIFT DRAG OF THE DOUGLAS
F5D-1 AIRPLANE AS OBTAINED WITH A 0.125-SCALE
ROCKET-BOOSTED MODEL BETWEEN MACH
NUMBERS OF 0.81 AND 1.64

TEED NO. NACA AD 399

By Earl C. Hastings, Jr., and Waldo L. Dickens

ABSTRACT

A flight investigation was conducted to determine the effects of inlet modification and rocket-rack extension on the longitudinal trim and low-lift drag of the Douglas F5D-1 airplane. The investigation was conducted with a 0.125-scale rocket-boosted model between Mach numbers of 0.81 and 1.64.

This paper presents the changes in trim angle of attack, trim lift coefficient, and low-lift drag caused by the modified inlets alone over a small part of the test Mach number range and by a combination of the modified inlets and extended rocket racks throughout the remainder of the test.

INDEX HEADINGS

Protuberances - Bodies	1.3.2.5
Stores - Airplane Components	1.7.1.1.5
Airplanes - Specific Types	1.7.1.2

NASA Technical Library



3 1176 01437 9300